

2.8 Million Years of Arctic Climate Change from Lake El'gygytgyn, NE Russia

Martin Melles,^{1*} Julie Brigham-Grette,² Pavel S. Minyuk,³ Norbert R. Nowaczyk,⁴ Volker Wennrich,¹ Robert M. DeConto,² Patricia M. Anderson,⁵ Andrei A. Andreev,¹ Anthony Coletti,² Timothy L. Cook,^{2†} Eeva Haltia-Hovi,^{4‡} Maaret Kukkonen,¹ Anatoli V. Lozhkin,³ Peter Rosén,⁶ Pavel Tarasov,⁷ Hendrik Vogel,¹ Bernd Wagner¹

¹Institute of Geology and Mineralogy, University of Cologne, Zulpicher Str. 49a, D-50674 Cologne, Germany.

²Department of Geosciences, University of Massachusetts, 611 North Pleasant Street, Amherst, MA 01003, USA.

³Far East Branch Russian Academy of Sciences, North-East Interdisciplinary Scientific Research Institute, 16 Portovaya St., 685000, Magadan, Russia.

⁴Helmholtz Centre Potsdam, GFZ German Research Centre for Geosciences, Telegrafenberg C321, D-14473 Potsdam, Germany.

⁵Earth & Space Sciences, University of Washington, Box 351310, Seattle, WA 98195-1310, USA.

⁶Climate Impacts Research Centre, Umeå University, SE-981 07 Abisko, Sweden.

⁷Institute of Geological Sciences, Free University Berlin, Malteserstr. 74-100, Haus D, D-12249 Berlin, Germany.

*To whom correspondence should be addressed. E-mail: mmelles@uni-koeln.de

†Present address: Department of Physical and Earth Sciences, Worcester State University, Worcester, MA 01602, USA.

‡ Present address: Department of Geology, Lund University, Sölvegatan 12, S-223 62, Lund, Sweden.

The reliability of Arctic climate predictions is currently hampered by insufficient knowledge of natural climate variability in the past. A sediment core from Lake El'gygytgyn (NE Russia) provides a continuous high-resolution record from the Arctic spanning the past 2.8 Ma. The core reveals numerous "super interglacials" during the Quaternary, with maximum summer temperatures and annual precipitation during marine benthic isotope stages (MIS) 11c and 31 ~4-5°C and ~300 mm higher than those of MIS 1 and 5e. Climate simulations show these extreme warm conditions are difficult to explain with greenhouse gas and astronomical forcing alone, implying the importance of amplifying feedbacks and far field influences. The timing of Arctic warming relative to West Antarctic Ice Sheet retreats implies strong interhemispheric climate connectivity.

The effects of global warming are documented and predicted to be most pronounced in the Arctic, a region which plays a crucial, but not yet well understood role within the global climate system (1). Reliable climate projections for high northern latitudes are, however, hampered by the complexity of the underlying natural variability and feedback mechanisms (2, 3). To date, information concerning the natural climate variability in the Arctic is widely restricted to the last glacial-interglacial cycle, the period covered by the longest ice-core records from the Greenland ice cap (4). A limited number of records extend deeper in time, both from the marine realm (5) and from the Arctic borderland (6), but these records are restricted in terms of age control and temporal resolution.

Here we present a time-continuous and high-resolution record of environmental history from the Arctic spanning the past 2.8 Ma, from Lake El'gygytgyn, located ~100 km to the north of the Arctic Circle in north-eastern Russia (67.5°N, 172°E, Fig. 1). The length, temporal continuity, and centennial to millennial-scale temporal resolution (Fig. 2 and sup-

plementary materials) provide a detailed view of natural climatic and environmental variability in the terrestrial Arctic, a better understanding of the representative nature of the last climate cycle for the Quaternary, and how sensitive the terrestrial Arctic reacts to a range of forcing mechanisms.

Lake setting, drilling, and core analyses. Lake El'gygytgyn is located in a meteorite impact crater formed 3.58 Ma ago (7). The 170 m deep lake has a bowl-shaped morphology with a diameter of ca. 12 km, a surface area of 110 km², and a relatively small catchment of 293 km² (8). The modern continental Arctic climate produces herb-dominated tundra in the catchment, nine months per year of lake-ice cover, and oligotrophic to ultra-oligotrophic conditions in the lake. Low productivity in combination with complete overturning of the water column during the ice-free period in summer leads to well-oxygenated bottom waters throughout the year.

Scientific deep drilling was performed in the El'gygytgyn Crater in winter 2008/09 (9). The core composite from Site 5011-1 (Fig. 1) of the International Continental Scientific Drilling Program (ICDP) was investigated for lithology as well as selected physical, chemical and biological proxies using advanced high-resolution (logging/scanning) technologies along with standard techniques (10). According to the age model (Fig. 2), which is based on magnetostratigraphy and tuning of proxy data to the regional insolation and global marine isotope stratigraphy (fig. S1), the upper 135.2 m of the sediment record continuously represents the environmental history of the past 2.8 Ma. To display the obtained data versus time (Fig. 3) volcanic ashes and other event layers caused by mass movement deposits were removed (10). While highly varied in nature, the resultant record of pelagic sedimentation consists of three dominant lithofacies (see supplementary materials). Climate and environmental interpretation of the pelagic sedimentation record is based on complementary biological and geochemical indicators, which show that distinct facies reflect end-member glacial-interglacial climatic conditions (9, 11).

Glacial variability and proxies. Facies A is characterized by dark gray to black, finely laminated (<5 mm) silt and clay and may contain elongated sediment clasts of coarser grain sizes (supplementary materials, fig. S2). This facies was deposited during times of heavy global marine isotopic values (12) and low regional July insolation (Fig. 3, A, B, D) (13). It represents peak glacial conditions, when perennial lake ice persisted, requiring mean annual air temperatures at least 4 (± 0.5) °C lower than today (14). This resulted in a stagnant water column with oxygen-depleted bottom waters, as reflected by low manganese/iron

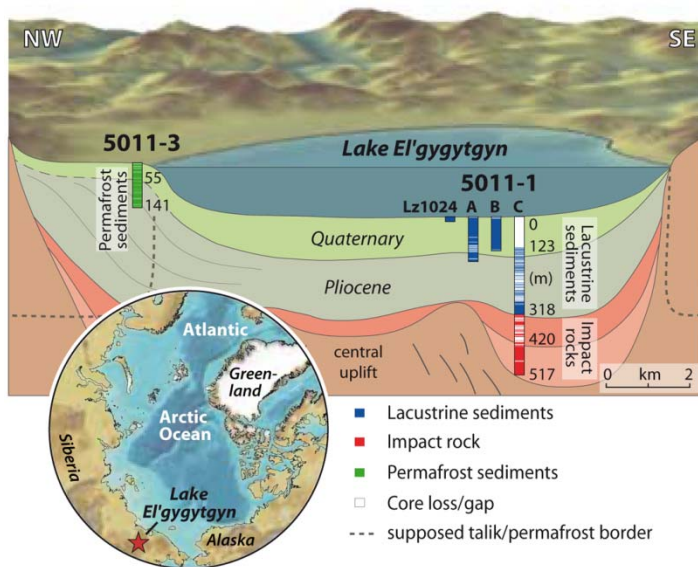


Fig. 1. Location of Lake El'gygytyn in northeastern Russia (inserted map) and schematic cross-section of the El'gygytyn basin stratigraphy showing the location of ICDP Sites 5011-1 and 5011-3. At Site 5011-1, three holes (1A, 1B, and 1C) were drilled to replicate the Quaternary and uppermost Pliocene sections. Hole 1C further penetrated through the remaining lacustrine sequence down to 318 m depth and then ~200 m into the impact rock sequence underneath. Lz1024 is a 16-m long percussion piston core taken in 2003 that fills the stratigraphic gap between the lake sediment surface and the top of drill cores 1A and 1B.

(Mn/Fe) ratios (Fig. 3G) and minima in magnetic susceptibility (MS) (Fig. 3E), indicating reducing conditions with magnetite dissolution (see supplementary materials). Dark laminations along with maxima in the content of total organic carbon (TOC) (Fig. 3F) reflect the absence of bioturbation and enhanced preservation of organic matter. Low silicon/titanium (Si/Ti) ratios (Fig. 3H) and a robust correlation between Si/Ti ratios and biogenic silica contents (see supplementary materials), however, suggest relatively low primary production.

Facies A first appears 2.602-2.598 Ma ago, during MIS 104 (Fig. 3D), corresponding with pollen assemblages that indicate a significant cooling at the Pliocene/Pleistocene boundary (see supplementary materials). This cooling coincides with distinct climatic deterioration at Lake Baikal (15), and may be associated with the poorly dated Okanaanean Glaciation in eastern Chukotka at the beginning of the Pleistocene (16). On the other hand, the first occurrence of Facies A at Lake El'gygytyn clearly postdates the onset of stratification across the western subarctic Pacific Ocean at 2.73 Ma, an event believed to have triggered the intensification of Northern Hemispheric glaciation (17). Hence, the onset of full glacial cycles in central Chukotka cannot directly be linked to changes in thermohaline circulation in the Pacific.

From the long-term succession of Facies A (Fig. 3D) and Mn/Fe ratios (Fig. 3G) pervasive glacial episodes at Lake El'gygytyn gradually increase in frequency from ~2.3 to ~1.8 Ma, eventually concurring with all glacial and several stadials reflected globally in stacked marine isotope records (12). The full establishment of glacial/interglacial cycles by ~1.8 Ma at Lake El'gygytyn coincides well with enhanced glacial erosion in British Columbia (18) and the onset of subpolar cooling in both hemispheres with an average bipolar temperature drop of 4 to 5°C due to

the emergence of the tropical Pacific cold tongue (19). Nevertheless, it clearly predates the Mid-Pleistocene Transition (MPT), when the dominance of 41 ka obliquity was globally replaced by the 100 ka cycle between 1.25 and 0.7 Ma ago (20).

Interglacial variability and proxies. Facies B is characterized by massive to faintly banded silt of olive gray to brownish colors (supplementary materials, fig. S2). This facies comprises the majority of sediment that accumulated in Lake El'gygytyn during the past 2.8 Ma, representing 79% of the Quaternary history (Fig. 3D). It reflects a wide range of glacial to interglacial settings and includes the style of modern sedimentation. As such, a seasonal ice cover promotes higher diatom productivity, as indicated by high Si/Ti ratios (Fig. 3H, see supplementary materials). TOC content, in contrast, is low (Fig. 3F), suggesting high organic matter decomposition due to oxygenation of bottom waters as a consequence of wind and density-driven mixing. Complete water-column ventilation is also indicated in the sediment colors, maxima in MS (Fig. 3E), and high Mn/Fe ratios (Fig. 3G). In addition, the lack of stratification indicates minor sediment homogenization by bioturbation.

Facies C consists of reddish-brown silt-sized sediment with distinct fine laminations (<5 mm; supplementary materials, fig. S2). This facies is irregularly distributed in the record compared to Facies A and B (Fig. 3D). It coincides with some periods of light values in the global marine isotope record and high regional July insolation (Fig. 3, A and B). The characteristics of Facies C suggest that it represents particularly warm interglacials. High Mn/Fe ratios (Fig. 3G) along with reddish-brown sediment colors imply well-oxygenated bottom waters. In contrast with Facies B, however, the sediments are distinctly laminated. This is traced back to a combination of factors including a particularly high primary production in spring and summer and anoxic bottom water conditions during winter stratification under a seasonal ice cover, which excludes bioturbation despite annual oxygenation. High primary production, presumably caused by a longer ice-free season and enhanced nutrient supply from the catchment relative to other interglacials, is indicated by exceptionally high Si/Ti ratios (Fig. 3H). Anoxic bottom water conditions during winter are implied by high TOC contents (Fig. 3F), reflecting high primary production and incomplete decomposition compared to Facies B, and variable MS values (Fig. 3E), reflecting partial dissolution of magnetite.

The described characteristics of Facies C are most pronounced for MIS 11c, 31, 49, 55, 77, 87, 91, and 93 (red bars in Fig. 3), suggesting that these interglacials represent unusual "super interglacials" in the Arctic throughout the Quaternary. The exceptional character of these interglacial conditions becomes evident based upon a comparison of MIS 1 and 5e (Facies B) with MIS 11c and 31 (super interglacials of Facies C), using additional biological proxies and pollen-based climate reconstructions (Fig. 3, I to L).

Sediments formed in Lake El'gygytyn during MIS 1 and 5e have Si/Ti ratios only slightly higher than those formed during glacial and stadial conditions of MIS 2, 5d, and 6 (Fig. 3K). Pollen data show distinct increases in tree and shrub pollen (Fig. 3L) and suggest that notably birch and alder shrubs dominated the vegetation (fig. S4). Pollen-based climate reconstructions (see supplementary materials) suggest that the mean temperature of the warmest month (MTWM; i.e., July) and the annual precipitation (PANN) during the peak of MIS 1 and MIS 5e were only ~1-2°C and, with one exception, ~50 mm higher than today, respectively (Fig. 3, I and J).

This is consistent with temperature reconstructions for the Holocene thermal maximum, which indicate +1.6 (±0.8) °C warming in the western Arctic (21) and +1.7 (±0.8) °C across the entire Arctic (3) relative to modern, confirming that Lake El'gygytyn records regional rather than just local climate change (14). Temperature reconstructions for the MIS 5e thermal maximum, in contrast, are more variable, indicating +5 (±1) °C across the entire Arctic, although with smaller anomalies reconstruct-

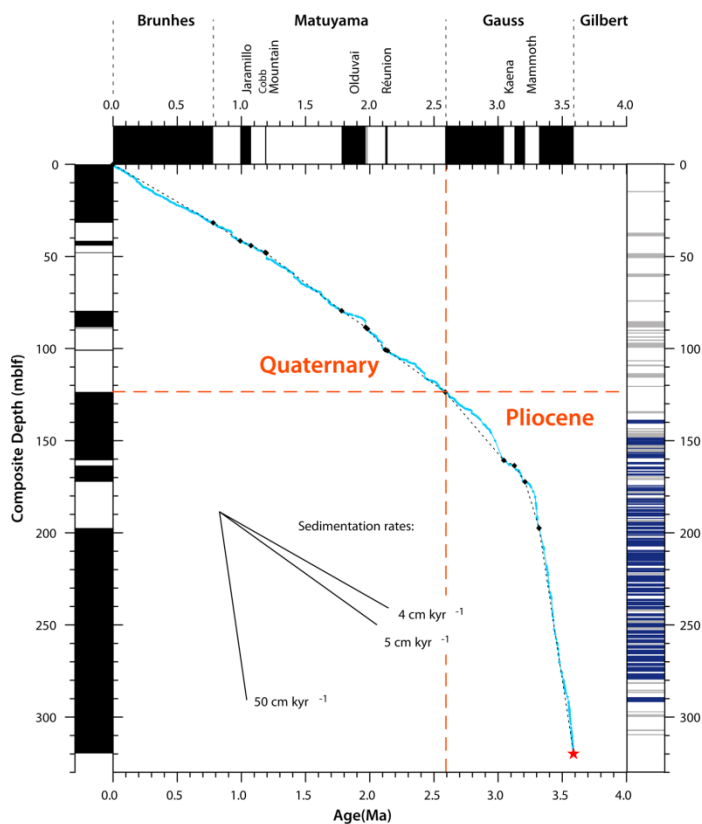


Fig. 2. Age/depth model with resulting sedimentation rates for the ICDP 5011-1 core composite based upon magnetostratigraphy and correlation between sediment proxy data, the LR04 marine isotope stack (12), and regional spring and summer insolation (13). Initial 1st order tie points are indicated by black diamonds, 2nd and 3rd order tie points by blue squares. The red star marks the time of the impact inferred from $^{40}\text{Ar}/^{39}\text{Ar}$ dating (7) at 3.58 (± 0.04) ka. Black and white bars denote normal and reversed polarity, respectively. Mass movement deposits and core gaps > 50 cm in thickness are indicated in the right bar with gray and blue colors, respectively.

ed for the Pacific sector (3, 22). The warmer climate across the Arctic during MIS 5e compared to MIS 1 is thought to have caused a size reduction of the Greenland Ice Sheet equivalent to 1.6-2.2 m in global sea-level rise (23).

Strongly enhanced primary productivity during the super interglacials MIS 11c and 31 compared to MIS 1 and 5e, as inferred from higher Si/Ti ratios (Fig. 3K), is associated with comparable maxima in tree and shrub pollen, but marked by distinct differences in pollen composition (Fig. 3L and supplementary materials). For instance, substantial spruce pollen is present during MIS 11c and 31, but is missing during shrub-dominated MIS 1 and 5e interglacials. According to the BMA (best modern analog) climate reconstruction, maximum MTWM and PANN were up to 4-5°C and ~300 mm higher than those of MIS 1 and 5e, respectively (Fig. 3, I and J).

Sediment records of MIS 11 are rare in the Arctic and their reconstructed temperature signals are inconclusive (22). However, there are indications that the Greenland Ice Sheet was much smaller or even absent (24, 25), with forests covering at least South Greenland (26). Rela-

tive sea level may have been significantly higher than today (25, 27). Particularly warm conditions are also suggested by records from Lake Biwa (28), Lake Baikal (29), the mid-latitude Atlantic (30), and the Belize Reef (31), and may have been associated with megadroughts in the southwestern USA (32).

MIS 31 as yet is not unambiguously recorded in the Arctic, but is known for significant changes in and around Antarctica, including a southward shift of the subtropical front and warmer waters in the Southern Ocean (33, 34), and the collapse of the West Antarctic Ice Sheet (WAIS) (35). In the Northern Hemisphere, the Plio/Pleistocene Gubik Formation of northern Alaska includes at least five high sea-level stands associated with episodes of warm climate and reduced sea ice (36). One of these episodes, the Fishcreekian transgression, is now thought to be ca. 1.2 Ma (37) and thus may be correlative with MIS 31. Another possibly correlative site is at Fosheim Dome on Ellesmere Island. This site includes terrestrial deposits dated to about 1.1 Ma, which enclose fossil beetle (Coleoptera) assemblages suggesting temperatures 8 to 14°C above modern values (38).

Other Arctic sites potentially correlative with one or more of the older Early Pleistocene super interglacials recorded in Lake El'gygytyn (Fig. 3) include the Kap København Formation in northern Greenland, currently dated to about 2.4 Ma. At this time, sea ice was strongly reduced and forests reached the Arctic Ocean about 1000 km further to the north than today (39). Another candidate is the balmy Bigbendian Transgression of the Gubik Formation dated to about 2.6 Ma (36).

Interglacial forcings and feedbacks. Comparing the relative warmth of the Pleistocene interglacials recorded at Lake El'gygytyn (Fig. 3I) in the context of orbital and greenhouse gas (GHG) forcing (40), we find that peak summer warmth during MIS 5e and MIS 31 corresponds to the congruence of high obliquity, high eccentricity, and precession aligning perihelion with boreal summer. The net effect of this orbital configuration produces high-intensity summer insolation at the lake, $>50 \text{ Wm}^{-2}$ greater than today (Fig. 3K). Similarly, peak warmth during MIS 1 and MIS 11c also coincides with perihelion during boreal summer, but lower eccentricity (and lower obliquity at MIS 11c) attenuates the effect of precession relative to MIS 5e and MIS 31, making summer insolation forcing less intense, albeit longer in duration.

GHG radiative forcing from a combination of CO_2 , CH_4 , and N_2O atmospheric mixing ratios determined from ice cores (see supplementary materials) is similar during MIS 5e and MIS 11c ($+0.16 \text{ Wm}^{-2}$ and $+0.19 \text{ Wm}^{-2}$ relative to pre-industrial GHG concentrations, respectively). Early MIS 1 is clearly an exception, with substantially lower CO_2 levels (~260 ppmv) around the time of peak Holocene warmth (~9 ka) producing -0.44 Wm^{-2} less radiative forcing relative to pre-industrial. MIS 31 (~1.072 Ma) lies beyond the oldest ice cores, so no direct information on atmospheric composition is available. However, a proxy-based reconstruction of mid-Pleistocene $p\text{CO}_2$ based on boron isotopes in planktonic foraminifera (41) indicates that the highest mid-Pleistocene CO_2 levels (~325 ppmv) occurred around 1 Ma, roughly coinciding with the exceptional warmth of MIS 31. While uncertain, these reconstructed CO_2 levels at MIS 31 would have added $\sim 0.84 \text{ Wm}^{-2}$ of radiative forcing, even if CH_4 and N_2O mixing levels remained close to pre-industrial values, which is unlikely considering the ubiquitous correlation of elevated CH_4 and N_2O during late Pleistocene interglacials. In sum, much of the warmth during MIS 31 can be explained by elevated greenhouse gas levels (42).

To investigate potential reasons for the super interglacials at Lake El'gygytyn, we tested the equilibrated response of a Global Climate Model (GCM) with an interactive vegetation component (see supplementary materials) to the orbital and greenhouse gas forcing corresponding to the timing of peak summer warmth at MIS 1, 5e, 11c, and 31. Comparisons with a pre-industrial control simulation (Fig. 4) show that differences in MTWM maxima at Lake El'gygytyn during MIS 1 and

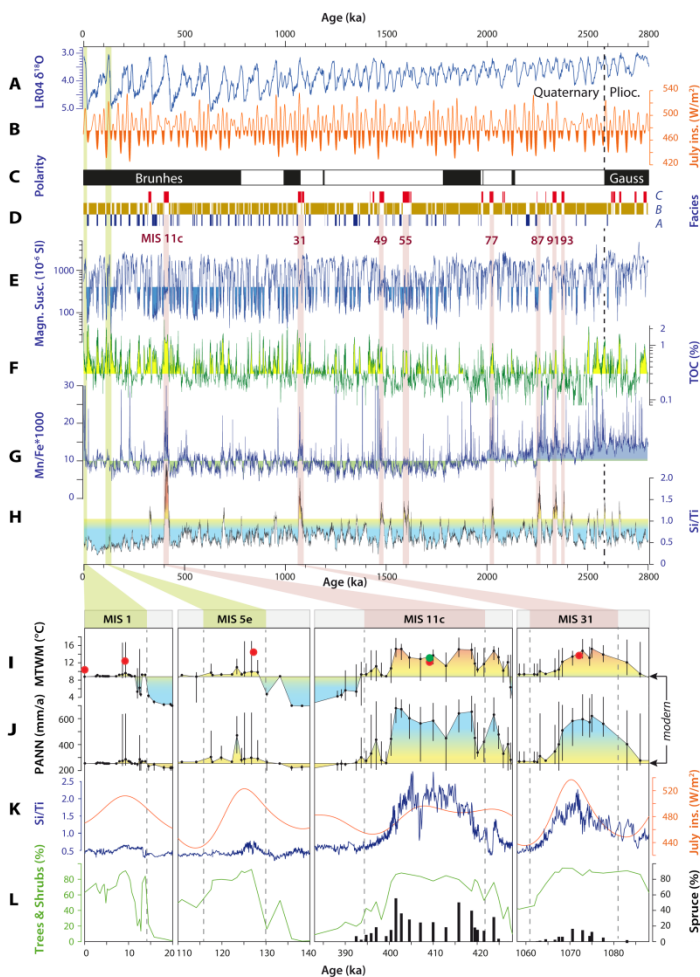


Fig. 3. Upper part: (A) LR04 global marine isotope stack (12) and (B) mean July insolation for 67.5°N (13) for the past 2.8 Ma compared to (C) magnetostratigraphy, (D) facies, (E) magnetic susceptibility, (F) TOC contents, (G) Mn/Fe ratios, and (H) Si/Ti ratios in the sediment record from Lake El'gygytyn (MS and XRF data are smoothed using a 500-year weighted running mean in order to improve the signal-to-noise ratio). Super interglacials at Lake El'gygytyn are highlighted with red bars. Lower part: Expanded views into the interglacials MIS 1, 5e, 11c, and 31 and adjoining glacials/stadials. (I) Reconstructed mean temperatures of the warmest month (MTWM) and (J) reconstructed annual precipitation (PANN) based on the pollen spectra and best modern analog approach [modern values from (56)]. (K) Mean July insolation for 67.5°N (13) compared to El'gygytyn Si/Ti ratios, smoothed by 5-point weighted running mean. (L) Tree and shrub pollen percentages compared to spruce pollen content. Simulated July surface air temperatures (red and green dots) at the location of the Lake are shown for comparison. The location of the dots relative to the x-axis corresponds with the GHG and orbital forcing used in each interglacial simulation (see supplementary materials). Simulated modern and pre-industrial temperatures are close to observed, so model temperatures are not bias corrected. The green dot indicates the results derived with a deglaciated Greenland and increased heat flux under Arctic Ocean sea ice by 8 W m^{-2} .

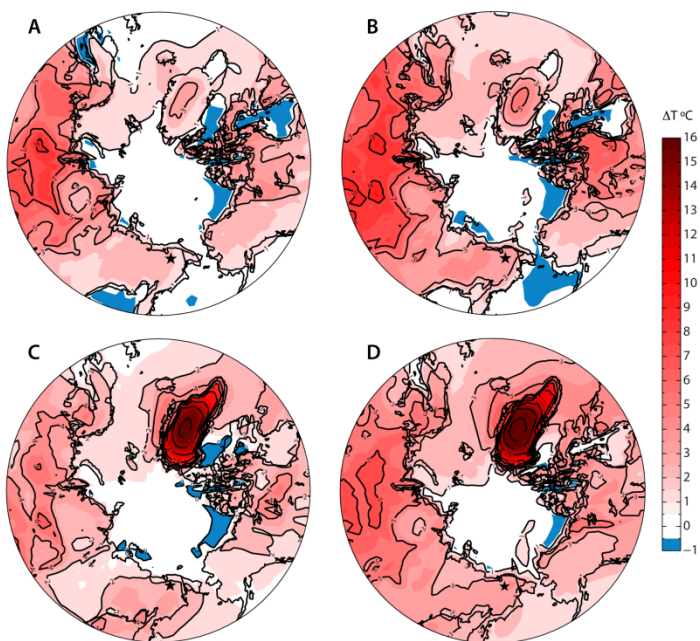


Fig. 4. Simulated interglacial warming (2-m surface temperature in °C) relative to pre-industrial. (A) MIS 1 (9 ka orbit and GHGs). (B) MIS 5e (127 ka orbit and GHGs). (C) MIS 11c (409 ka orbit, GHGs, no Greenland Ice Sheet, and 8 W m^{-2} enhanced oceanic heat convergence under Arctic sea ice). (D) MIS 31 (1072 ka orbit, GHGs, and no Greenland Ice Sheet). Orbital and GHG forcing for MIS 5e and 11c follow that used in (40). Forcing for MIS 31 follows that used by (42). The location of Lake El'gygytyn is shown with a star near the bottom-center of each panel. Areas of no shading (white) roughly correspond to statistically insignificant anomalies at the 95% confidence interval.

5e (+2.1 and +4.2°C) were in the same range as those during MIS 11c and 31 (+2.2 and +3.5°C) (Fig. 3I, red dots, Fig. 4, and supplementary materials). The same holds true for the modeled differences in PANN (0 and -37 mm/a, and +38 and 0 mm/a, respectively). The results are similar to previous interglacial simulations using an intermediate complexity model (40), with the combined effect of orbital and GHG forcing at MIS 5e producing the greatest summer warming among the four interglacials modeled here. Our simulated summer warming (4.2°C) over the Beringian interior at MIS 5e also closely matches the warming simulated by a coupled atmosphere-ocean GCM (43). Consequently, the distinctly higher observed values of MTWM and PANN at MIS 11c cannot readily be explained by the local summer orbital forcing or GHG concentrations alone, and suggest that other processes and feedbacks contributed to the extraordinary warmth at this interglacial, and the relatively muted response to the strongest forcing at MIS 5e.

Vegetation-land surface feedbacks are accounted for in our model, and the simulated poleward advance of evergreen needle-leaf forest during the interglacials provides a good match with our reconstructions (see supplementary materials), yet the warming effect of boreal forest expansion does not provide a satisfactory explanation for the warmth of MIS 11c. A deglaciated Greenland has been shown to have important regional effects on surrounding sea surface temperatures (SSTs) and sea ice conditions, but widespread warming in the circum-Arctic (and Beringia in particular) has been shown to be minimal (43, 44). This is supported by our simulations, showing that the loss of the Greenland Ice Sheet at MIS 11c raises summer temperatures at Lake El'gygytyn by only 0.3°C. Furthermore, Greenland was likely reduced in size during MIS 5e and perhaps other interglacials, offering little help in differentiating Beringia's response from one interglacial to the next. Meltwater impacts on ocean overturning (ignored in our simulations) generally have a cooling effect on the Northern Hemisphere, adding to the difficulty in explaining the exceptional warmth at MIS 11c relative to MIS 1 and 5e.

The super interglacials at Lake El'gygytyn coincide remarkably with diatomite layers in the Antarctic ANDRILL 1B record (see supplementary materials), which reflect periods of a diminished West Antarctic Ice Sheet (WAIS) and open water in the Ross Embayment (35, 45). The higher number of events at Lake El'gygytyn does not necessarily reflect a higher frequency, but could also reflect the discontinuity of the ANDRILL 1B record (46).

Linkages between extraordinary warmth at Lake El'gygytyn and Antarctic ice volume imply strong intra-hemispheric climate coupling that could be related to reductions in Antarctic Bottom Water (AABW) formation (47) during times of ice sheet/shelf retreat and elevated fresh water input into the Southern Ocean. This is supported by distinct minima in AABW inflows into the southwest Pacific during MIS 11 and MIS 31 (48). As a consequence, changes in thermohaline circulation (THC) during MIS 11 and MIS 31 might have reduced upwelling in the northern North Pacific (49), as indicated by distinctly lower BSi concentrations compared to other interglacials at ODP Site 882 (50, 51). A stratified water column during the super interglacials would have resulted in higher sea surface temperatures in the northern North Pacific, with the potential to raise air temperatures and precipitation rates over adjacent land masses via effects on the dominant pressure patterns (Siberian High and Aleutian Low) that dominate the modern climatology at the lake (52).

An alternative mechanism linking Lake El'gygytyn with Antarctica could be related to higher relative sea level due to the combined retreats of the WAIS (44) and the Greenland Ice Sheet (24), resulting in enhanced warm-water intrusion into the Arctic Ocean. Potential gateways are the Denmark Strait and Barents Sea from the Atlantic Ocean and the Bering Strait from the Pacific Ocean. In the northeastern Atlantic, however, SSTs at least during MIS 11 were lower than during MIS 9, 5e, and 1 (53). Bering Strait throughflow today is restricted by shallow waters of

only ~50 m depth, resulting in an average northward transport of ~0.8 Sv ($1 \text{ Sv} = 10^6 \text{ m}^3 \text{ s}^{-1}$) (54). Substantial interannual variability in flow rate can produce elevated heat fluxes ($5\text{--}6 \times 10^{20} \text{ J/yr}$ in 2007), which can be amplified in the Arctic by internal feedback mechanisms (3). No evidence as yet exists for substantial changes in temperature or flow rates during super interglacials, however, as a first exploration of this idea, we increased the heat flux convergence under Arctic sea ice in our interglacial climate model simulations by 8 W m^{-2} (reflecting an extreme ~4-fold increase in warmer Bering Strait throughflow). The additional heat flux results in substantial reductions in seasonal sea ice and warmer Arctic SSTs, but contributes little additional warming ($<0.7^\circ\text{C}$; Figs. 3I and 4C) in the Beringian interior.

Fully testing these ideas will require additional climate-ocean modeling, explicitly accounting for glacial-interglacial changes in regional sea level (paleobathymetry and gateways), changes in land-ice distributions, and melt-water inputs in both polar regions, as well as contemporaneous sediment records from the Arctic and North Pacific Oceans.

The paleoclimatic record from Lake El'gygytyn provides a benchmark of Arctic change from an area that has otherwise been a data desert for time-continuous terrestrial records of the Pliocene and Pleistocene. The sediments provide a fresh window into the environmental dynamics of the Arctic from a terrestrial high latitude site for comparison with other Arctic records. Marine cores from the Arctic basin, such as those from the ACEX/Lomonosov Ridge or HOTRAX expeditions [(55) and references therein] still lack the comparable resolution and length to test for perennial versus seasonal sea ice conditions during interglacials over the past 2.8 Ma. The attenuated response of Arctic SSTs in model simulations of the interglacials (Fig. 4) (43) relative to surrounding continents hints that deep Arctic Ocean cores might not provide a complete perspective of the pacing or magnitude of climate change in the Arctic borderlands. The observed response of the region's climate and terrestrial ecosystems to a range of interglacial forcing provides a challenge for modeling and important constraints on climate sensitivity and polar amplification. The remarkable coherence of interglacial warmth across the western Arctic with repeated deglaciation events in West Antarctica supports the notion of strong teleconnections between the polar regions over the last 2.8 million years.

References and Notes

1. ACIA, *Arctic Climate Impact Assessment* (Cambridge Univ. Press, Cambridge, 2005).
2. J. Christensen *et al.*, in *Fourth Assessment Report of the Intergovernmental Panel on Climate Change* (Cambridge Univ. Press, Cambridge, 2007), pp. 847–940.
3. G. H. Miller *et al.*, Arctic amplification: Can the past constrain the future? *Quat. Sci. Rev.* **29**, 1779 (2010). doi:10.1016/j.quascirev.2010.02.008
4. North Greenland Ice Core Project members, High-resolution record of Northern Hemisphere climate extending into the last interglacial period. *Nature* **431**, 147 (2004). doi:10.1038/nature02805 Medline
5. M. O'Regan, C. J. Williams, K. E. Frey, M. Jakobsson, A synthesis of the long-term paleo-climatic evolution of the Arctic. *Oceanography* **24**, 66 (2011). doi:10.5670/oceanog.2011.57
6. CAPE Last Interglacial Project Members, Last interglacial Arctic warmth confirms polar amplification of climate change. *Quat. Sci. Rev.* **25**, 1383 (2006). doi:10.1016/j.quascirev.2006.01.033
7. P. Layer, Argon-40/argon-39 age of the El'gygytyn impact event, Chukotka, Russia. *Meteorit. Planet. Sci.* **35**, 591 (2000). doi:10.1111/j.1945-5100.2000.tb01439.x
8. M. Nolan, J. Brigham-Grette, Basic hydrology, limnology, and meteorology of modern Lake El'gygytyn, Siberia. *J. Paleolimnol.* **37**, 17 (2007). doi:10.1007/s10933-006-9020-y
9. M. Melles *et al.*, The El'gygytyn Scientific Drilling Project – conquering Arctic challenges through continental drilling. *Sci. Drill.* **11**, 29 (2011).
10. Materials and methods are available as supplementary materials on Science Online.

11. M. Melles *et al.*, Sedimentary geochemistry of core PG1351 from Lake El'gygytgyn Lake—A sensitive record of climate variability in the East Siberian Arctic during the past three glacial-interglacial cycles. *J. Paleolimnol.* **37**, 89 (2007). [doi:10.1007/s10933-006-9025-6](https://doi.org/10.1007/s10933-006-9025-6)
12. L. E. Lisiecki, M. E. Raymo, A Pliocene-Pleistocene stack of 57 globally distributed benthic $\delta^{18}\text{O}$ records. *Paleoceanography* **20**, PA1003 (2005). [doi:10.1029/2004PA001071](https://doi.org/10.1029/2004PA001071)
13. J. Laskar *et al.*, A long-term numerical solution for the insolation quantities of the Earth. *Astron. Astrophys.* **428**, 261 (2004). [doi:10.1051/0004-6361:20041335](https://doi.org/10.1051/0004-6361:20041335)
14. M. Nolan, Analysis of local AWS and NCEP/NCAR reanalysis data at Lake El'gygytgyn, and its implications for maintaining multi-year lake-ice covers. *Clim. Past Disc.* **8**, 1443 (2012). [doi:10.5194/cpd-8-1443-2012](https://doi.org/10.5194/cpd-8-1443-2012)
15. D. Demske, B. Mohr, H. Oberhänsli, Late Pliocene vegetation and climate of the Lake Baikal region, southern East Siberia, reconstructed from palynological data. *Palaeogeogr. Palaeoclimatol. Palaeoecol.* **184**, 107 (2002). [doi:10.1016/S0031-0182\(02\)00251-1](https://doi.org/10.1016/S0031-0182(02)00251-1)
16. A. F. Fradkina *et al.*, Northeastern Asia. *Spec. Pap. Geol. Soc. Am.* **382**, 105 (2005).
17. G. H. Haug *et al.*, North Pacific seasonality and the glaciation of North America 2.7 million years ago. *Nature* **433**, 821 (2005). [doi:10.1038/nature03332](https://doi.org/10.1038/nature03332) [Medline](#)
18. D. L. Shuster, T. A. Ehlers, M. E. Rusmoren, K. A. Farley, Rapid glacial erosion at 1.8 Ma revealed by $^4\text{He}/^3\text{He}$ thermochronometry. *Science* **310**, 1668 (2005). [doi:10.1126/science.1118519](https://doi.org/10.1126/science.1118519) [Medline](#)
19. A. Martínez-García, A. Rosell-Meléndez, E. L. McClymont, R. Gersonde, G. H. Haug, Subpolar link to the emergence of the modern equatorial Pacific cold tongue. *Science* **328**, 1550 (2010). [doi:10.1126/science.1184480](https://doi.org/10.1126/science.1184480) [Medline](#)
20. P. U. Clark *et al.*, The middle Pleistocene transition: Characteristics, mechanisms, and implications for long-term changes in atmospheric pCO₂. *Quat. Sci. Rev.* **25**, 3150 (2006). [doi:10.1016/j.quascirev.2006.07.008](https://doi.org/10.1016/j.quascirev.2006.07.008)
21. D. S. Kaufman, J. Brigham-Grette, Aminostratigraphic correlations and paleotemperature implications, Pliocene-Pleistocene high-sea-level deposits, northwestern Alaska. *Quat. Sci. Rev.* **12**, 21 (1993). [doi:10.1016/0277-3791\(93\)90046-O](https://doi.org/10.1016/0277-3791(93)90046-O)
22. G. H. Miller *et al.*, Temperature and precipitation history of the Arctic. *Quat. Sci. Rev.* **29**, 1679 (2010). [doi:10.1016/j.quascirev.2010.03.001](https://doi.org/10.1016/j.quascirev.2010.03.001)
23. E. J. Colville *et al.*, Sr-Nd-Pb isotope evidence for ice-sheet presence on southern Greenland during the Last Interglacial. *Science* **333**, 620 (2011). [doi:10.1126/science.1204673](https://doi.org/10.1126/science.1204673) [Medline](#)
24. E. Willerslev *et al.*, Ancient biomolecules from deep ice cores reveal a forested southern Greenland. *Science* **317**, 111 (2007). [doi:10.1126/science.1141758](https://doi.org/10.1126/science.1141758) [Medline](#)
25. M. E. Raymo, J. X. Mitrovica, Collapse of polar ice sheets during the stage 11 interglacial. *Nature* **483**, 453 (2012). [doi:10.1038/nature10891](https://doi.org/10.1038/nature10891) [Medline](#)
26. A. de Vernal, C. Hillaire-Marcel, Natural variability of Greenland climate, vegetation, and ice volume during the past million years. *Science* **320**, 1622 (2008). [doi:10.1126/science.1153929](https://doi.org/10.1126/science.1153929) [Medline](#)
27. G. A. Milne, J. X. Mitrovica, Searching for eustasy in deglacial sea-level histories. *Quat. Sci. Rev.* **27**, 2292 (2008). [doi:10.1016/j.quascirev.2008.08.018](https://doi.org/10.1016/j.quascirev.2008.08.018)
28. P. E. Tarasov *et al.*, Progress in the reconstruction of Quaternary climate dynamics in the Northwest Pacific: a new modern analogue reference dataset and its application to the 430-kyr pollen record from Lake Biwa. *Earth Sci. Rev.* **108**, 64 (2011). [doi:10.1016/j.earscirev.2011.06.002](https://doi.org/10.1016/j.earscirev.2011.06.002)
29. A. A. Prokopenko *et al.*, Climate in continental interior Asia during the longest interglacial of the past 500 000 years: The new MIS 11 records from Lake Baikal, SE Siberia. *Clim. Past* **6**, 31 (2010). [doi:10.5194/cp-6-31-2010](https://doi.org/10.5194/cp-6-31-2010)
30. R. Stein, J. Heffter, J. Grützner, A. Voelker, B. D. A. Naafs, Variability of surface water characteristics and Heinrich-like events in the Pleistocene midlatitude North Atlantic Ocean: biomarker and XRD records from IODP Site U1313 (MIS 16-9). *Paleoceanography* **24**, PA2203 (2009). [doi:10.1029/2008PA001639](https://doi.org/10.1029/2008PA001639)
31. E. Gischler, R. N. Ginsburg, J. O. Herrle, S. Prasad, Mixed carbonates and siliciclastics in the Quaternary of southern Belize: Pleistocene turning points in reef development controlled by sea-level change. *Sedimentology* **57**, 1049 (2010). [doi:10.1111/j.1365-3091.2009.01133.x](https://doi.org/10.1111/j.1365-3091.2009.01133.x)
32. P. J. Fawcett *et al.*, Extended megadroughts in the southwestern United States during Pleistocene interglacials. *Nature* **470**, 518 (2011). [doi:10.1038/nature09839](https://doi.org/10.1038/nature09839) [Medline](#)
33. R. P. Scherer *et al.*, Antarctic records of precession-paced insolation-driven warming during early Pleistocene Marine Isotope Stage 31. *Geophys. Res. Lett.* **35**, L03505 (2008). [doi:10.1029/2007GL032254](https://doi.org/10.1029/2007GL032254)
34. P. Maiorano, M. Marino, J.-A. Flores, The warm interglacial Marine Isotope Stage 31: Evidences from the calcareous nanofossil assemblages at Site 1090 (Southern Ocean). *Mar. Micropaleontol.* **71**, 166 (2009). [doi:10.1016/j.marmicro.2009.03.002](https://doi.org/10.1016/j.marmicro.2009.03.002)
35. T. Naish *et al.*, Obliquity-paced Pliocene West Antarctic ice sheet oscillations. *Nature* **458**, 322 (2009). [doi:10.1038/nature07867](https://doi.org/10.1038/nature07867) [Medline](#)
36. J. Brigham-Grette, L. D. Carter, Pliocene marine transgressions of northern Alaska - circumarctic correlations and paleoclimate. *Arctic* **43**, 74 (1992).
37. G. A. Goodfriend, J. Brigham-Grette, G. H. Miller, Enhanced age resolution of the marine quaternary record in the Arctic using aspartic acid racemization dating of bivalve shells. *Quat. Res.* **45**, 176 (1996). [doi:10.1006/qres.1996.0018](https://doi.org/10.1006/qres.1996.0018)
38. S. A. Elias, J. V. Matthews Jr., Arctic North American seasonal temperatures from the latest Miocene to the Early Pleistocene, based on mutual climatic range analysis of fossil beetle assemblages. *Can. J. Earth Sci.* **39**, 911 (2002). [doi:10.1139/e01-096](https://doi.org/10.1139/e01-096)
39. S. Funder *et al.*, Late Pliocene Greenland – the Kap København Formation in North Greenland. *Bull. Geol. Soc. Den.* **48**, 177 (2001).
40. Q. Z. Yin, A. Berger, Individual contribution of insolation and CO₂ to the diversity of the interglacial climates of the past 800,000 years. *Clim. Dyn.* **36**, 1 (2011).
41. B. Hönisch, N. G. Hemming, D. Archer, M. Siddall, J. F. McManus, Atmospheric carbon dioxide concentration across the mid-Pleistocene transition. *Science* **324**, 1551 (2009). [doi:10.1126/science.1171477](https://doi.org/10.1126/science.1171477) [Medline](#)
42. R. M. DeConto, D. Pollard, D. Kowalewski, Modeling Antarctic ice sheet and climate variations during Marine Isotope Stage 31. *Global Planet. Change* **88-89**, 45 (2012). [doi:10.1016/j.gloplacha.2012.03.003](https://doi.org/10.1016/j.gloplacha.2012.03.003)
43. B. L. Otto-Bliesner, S. J. Marshall, J. T. Overpeck, G. H. Miller, A. Hu, Simulating Arctic climate warmth and icefield retreat in the last interglaciation. *Science* **311**, 1751 (2006). [doi:10.1126/science.1120808](https://doi.org/10.1126/science.1120808) [Medline](#)
44. S. J. Koenig, R. M. DeConto, D. Pollard, Late Pliocene to Pleistocene sensitivity of the Greenland Ice Sheet in response to external forcing and internal feedbacks. *Clim. Dyn.* **37**, 1247 (2011). [doi:10.1007/s00382-011-1050-0](https://doi.org/10.1007/s00382-011-1050-0)
45. D. Pollard, R. M. DeConto, Modelling West Antarctic ice sheet growth and collapse through the past five million years. *Nature* **458**, 329 (2009). [doi:10.1038/nature07809](https://doi.org/10.1038/nature07809) [Medline](#)
46. R. McKay *et al.*, Pleistocene variability of Antarctic Ice Sheet extent in the Ross Embayment. *Quat. Sci. Rev.* **34**, 93 (2012). [doi:10.1016/j.quascirev.2011.12.012](https://doi.org/10.1016/j.quascirev.2011.12.012)
47. A. Foldvik, Ice shelf water overflow and bottom water formation in the southern Weddell Sea. *J. Geophys. Res.* **109**, C02015 (2004). [doi:10.1029/2003JC002008](https://doi.org/10.1029/2003JC002008)
48. I. R. Hall, I. N. McCave, N. J. Shackleton, G. P. Weedon, S. E. Harris, Intensified deep Pacific inflow and ventilation in Pleistocene glacial times. *Nature* **412**, 809 (2001). [doi:10.1038/35090552](https://doi.org/10.1038/35090552) [Medline](#)
49. E. D. Galbraith *et al.*, Carbon dioxide release from the North Pacific abyss during the last deglaciation. *Nature* **449**, 890 (2007). [doi:10.1038/nature06227](https://doi.org/10.1038/nature06227) [Medline](#)
50. G. H. Haug, M. A. Maslin, M. Sarnthein, R. Stax, R. Tiedemann, Evolution of northwest Pacific sedimentation patterns since 6 Ma (Site 882). *Proc. ODP, Sci. Results* **145**, 293-314 (1995).
51. S. L. Jaccard, E. D. Galbraith, D. M. Sigman, G. H. Haug, A pervasive link between Antarctic ice core and subarctic Pacific sediment records over the past 800 kyr. *Quat. Sci. Rev.* **29**, 206 (2010). [doi:10.1016/j.quascirev.2009.10.007](https://doi.org/10.1016/j.quascirev.2009.10.007)
52. C. J. Mock, P. J. Bartlein, P. A. Anderson, Atmospheric circulation patterns and spatial climatic variations in Beringia. *Int. J. Climatol.* **18**, 1085 (1998). [doi:10.1002/\(SICI\)1097-0088\(199808\)18:10<1085::AID-JOC305>3.0.CO;2-K](https://doi.org/10.1002/(SICI)1097-0088(199808)18:10<1085::AID-JOC305>3.0.CO;2-K)
53. J. P. Helmke, H. A. Bauch, Comparison of glacial and interglacial conditions between the polar and subpolar North Atlantic region over the last five climatic cycles. *Paleoceanography* **18**, 1036 (2003). [doi:10.1029/2002PA000794](https://doi.org/10.1029/2002PA000794)

54. R. A. Woodgate, T. Weingartner, R. Lindsay, The 2007 Bering Strait oceanic heat flux and anomalous Arctic sea-ice retreat. *Geophys. Res. Lett.* **37**, L01602 (2010). doi:10.1029/2009GL041621
55. L. Polyak, M. Jakobsson, Quaternary sedimentation in the Arctic Ocean - recent advances and further challenges. *Oceanography* **24**, 52 (2011). doi:10.5670/oceanog.2011.55
56. M. New, D. Lister, M. Hulme, I. Makin, A high-resolution data set of surface climate over global land areas. *Clim. Res.* **21**, 1 (2002). doi:10.3354/cr021001
57. A. C. Gebhardt, F. Niessen, C. Kopsch, Central ring structure identified in one of the world's best-preserved impact craters. *Geology* **34**, 145 (2006). doi:10.1130/G22278.1
58. G. Schwamborn, G. Fedorov, L. Schirrmeister, H. Meyer, H.-W. Hubberten, Periglacial sediment variations controlled by late Quaternary climate and lake level change at Elgygytyn Crater, Arctic Siberia. *Boreas* **37**, 55 (2008). doi:10.1111/j.1502-3885.2007.00011.x
59. O. Juschus, M. Melles, A. C. Gebhardt, F. Niessen, Late Quaternary mass movement events in Lake El'gygytyn, northeastern Siberia. *Sedimentology* **56**, 2155 (2009). doi:10.1111/j.1365-3091.2009.01074.x
60. J. L. Kirschvink, The least-squares line and plane and the analysis of palaeomagnetic data. *Geophys. J. R. Astron. Soc.* **62**, 699 (1980). doi:10.1111/j.1365-246X.1980.tb02601.x
61. L. Löwemark *et al.*, Normalizing XRF-scanner data: A cautionary note on the interpretation of high-resolution records from organic-rich lakes. *J. Asian Earth Sci.* **40**, 1250 (2011). doi:10.1016/j.jseas.2010.06.002
62. H. Guyard *et al.*, High-altitude varve records of abrupt environmental changes and mining activity over the last 4000 years in the western French Alps (Lake Bramant, Grandes Rousses Massif). *Quat. Sci. Rev.* **26**, 2644 (2007). doi:10.1016/j.quascirev.2007.07.007
63. P. Rosén *et al.*, Universally applicable model for the quantitative determination of lake sediment composition using fourier transform infrared spectroscopy. *Environ. Sci. Technol.* **45**, 8858 (2011). doi:10.1021/es200203z Medline
64. PALE Steering Committee, Research protocols for PALE: Paleoclimate of Arctic Lakes and Estuaries, *PAGES Workshop Report Series 94-1*, 53 pp. (1994).
65. M. Davis, Determination of absolute pollen frequency. *Ecology* **47**, 310 (1966). doi:10.2307/1933780
66. E. C. Grimm, *TGView* (Illinois State Mus., Res. Collection Center, Springfield, 2004).
67. E. A. Mankinen, J. M. Donnelly, C. S. Grommé, Geomagnetic polarity event recorded at 1.1 m.y. B.P. on Cobb Mountain, Clear Lake volcanic field. *Calif. Geol.* **6**, 653 (1978).
68. J. E. T. Channell, D. A. Hodell, C. Xuan, A. Mazaud, J. S. Stoner, Age calibrated relative paleointensity for the last 1.5 Myr at IODP Site U1308 (North Atlantic). *Earth Planet. Sci. Lett.* **274**, 59 (2008). doi:10.1016/j.epsl.2008.07.005
69. J. E. T. Channell, J. Labs, M. E. Raymo, The Réunion subchronone at ODP site 981 (Feni Drift, North Atlantic). *Earth Planet. Sci. Lett.* **215**, 1 (2003). doi:10.1016/S0012-821X(03)00435-7
70. A. K. Baksi, K. A. Hoffman, M. McWilliams, Testing the accuracy of the geomagnetic polarity time-scale (GPTS) at 2-5 Ma, utilizing ⁴⁰Ar/³⁹Ar incremental heating data on whole-rock basalts. *Earth Planet. Sci. Lett.* **118**, 135 (1993). doi:10.1016/0012-821X(93)90164-5
71. X. Quidelleur, J. W. Holt, T. Salvany, H. Bouquerel, New K-Ar ages from La Montagne massif, Réunion Island (Indian Ocean), supporting two geomagnetic events in the time period 2.2-2.0 Ma. *Geophys. J. Int.* **182**, 699 (2010). doi:10.1111/j.1365-246X.2010.04651.x
72. J. G. Ogg, A. G. Smith, in *A Geologic Time Scale*, F. M. Gradstein, J. G. Ogg, A. G. Smith, Eds. (Cambridge Univ. Press, 2004), pp. 63-86.
73. A. A. Prokopenko, G. K. Khursevich, Plio-Pleistocene transition in the continental record from Lake Baikal: Diatom biostratigraphy and age model. *Quat. Int.* **219**, 26 (2010). doi:10.1016/j.quaint.2009.09.027
74. J. T. Overpeck, T. Webb III, I. C. Prentice, Quantitative interpretation of fossil pollen spectra: Dissimilarity coefficients and the method of modern analogs. *Quat. Res.* **23**, 87 (1985). doi:10.1016/0033-5894(85)90074-2
75. J. Guiot, Methodology of the last climatic cycle reconstruction in France from pollen data. *Palaeogeogr. Palaeoclimatol. Palaeoecol.* **80**, 49 (1990). doi:10.1016/0031-0182(90)90033-4
76. P. E. Tarasov *et al.*, Quantitative reconstruction of the Last Interglacial vegetation and climate based on the pollen record from Lake Baikal, Russia. *Clim. Dyn.* **25**, 625 (2005). doi:10.1007/s00382-005-0045-0
77. T. Nakagawa, P. E. Tarasov, K. Nishida, K. Gotanda, Y. Yasuda, Quantitative pollen-based climate reconstruction in central Japan: Application to surface and late Quaternary spectra. *Quat. Sci. Rev.* **21**, 2099 (2002). doi:10.1016/S0277-3791(02)00014-8
78. Polation (version 1.1) and Polygon (version 2.3.3) computer programs, <http://dendro.naruto-u.ac.jp/~nakagawa/> (2012).
79. C2 computer program, version 1.7.2, www.staff.ncl.ac.uk/staff/stephen.juggins/software/C2Home.htm (2012).
80. S. L. Thompson, D. Pollard, Greenland and Antarctic mass balances for present and doubled atmospheric CO₂ from the GENESIS Version-2 Global Climate Model. *J. Clim.* **10**, 871 (1997). doi:10.1175/1520-0442(1997)010<0871:GAAMBF>2.0.CO;2
81. L. O. Kaplan *et al.*, Climate change and Arctic ecosystems: 2. Modeling, paleodata-model comparisons, and future projections. *J. Geophys. Res.* **108**, 8171 (2003). doi:10.1029/2002JD002559
82. A. V. Lozhkin, P. M. Anderson, T. V. Matrosova, P. S. Minyuk, The pollen record from El'gygytyn Lake: Implications for vegetation and climate histories of northern Chukotka since the late middle Pleistocene. *J. Paleolimnol.* **37**, 135 (2007). doi:10.1007/s10933-006-9018-5
83. J. T. Kiehl *et al.*, The National Center for Atmospheric Research Community Climate Model: CCM3. *J. Clim.* **11**, 1131 (1998). doi:10.1175/1520-0442(1998)011<1131:TNCFAR>2.0.CO;2
84. D. Lüthi *et al.*, High-resolution carbon dioxide concentration record 650,000-800,000 years before present. *Nature* **453**, 379 (2008). doi:10.1038/nature06949 Medline
85. L. Loulergue *et al.*, Orbital and millennial-scale features of atmospheric CH₄ over the past 800,000 years. *Nature* **453**, 383 (2008). doi:10.1038/nature06950 Medline
86. A. Schilt *et al.*, Glacial-interglacial and millennial-scale variations in the atmospheric nitrous oxide concentration during the last 800,000 years. *Quat. Sci. Rev.* **29**, 182 (2010). doi:10.1016/j.quascirev.2009.03.011
87. A. Berger, Long-term variations of daily insolation and Quaternary climatic changes. *J. Atmos. Sci.* **35**, 2362 (1978). doi:10.1175/1520-0469(1978)035<2362:LTVOVI>2.0.CO;2
88. V. Ramaswamy *et al.*, in *Climate Change 2001: The Scientific Basis*, J. T. Houghton *et al.*, Eds. (Cambridge Univ. Press, Cambridge, 2001), pp. 349-426.
89. G. Shi, Radiative forcing and greenhouse effect due to the atmospheric trace gasses. *Sci. China (Series B)* **35**, 217 (1992).
90. A. Berger, M. Loutre, Insolation values for the climate of the last 10 million years. *Quat. Sci. Rev.* **10**, 297 (1991). doi:10.1016/0277-3791(91)90033-Q
91. M. Sturm, in *Moraines and Varves*, C. Schlüchter, Ed. (A. A. Balkema, Rotterdam, 1979), pp. 281-285.
92. S. M. Jepsen, E. E. Adams, J. C. Prisco, Sediment melt-migration dynamics in perennial Antarctic lake ice. *Arct. Antarct. Alp. Res.* **42**, 57 (2010). doi:10.1657/1938-4246-42.1.57
93. J. D. Tomkins, S. F. Lamoureux, D. Antoniades, W. F. Vincent, Sedimentary pellets as an ice-cover proxy in a High Arctic ice-covered lake. *J. Paleolimnol.* **41**, 225 (2009). doi:10.1007/s10933-008-9255-x
94. N. R. Nowaczyk, M. Melles, P. Minyuk, A revised age model for core PG1351 from Lake El'gygytyn, Chukotka, based on magnetic susceptibility variations tuned to northern hemisphere insolation variations. *J. Paleolimnol.* **37**, 65 (2007). doi:10.1007/s10933-006-9023-8
95. W. Davison, Iron and manganese in lakes. *Earth Sci. Rev.* **34**, 119 (1993). doi:10.1016/0012-8252(93)90029-7
96. J.-L. Loizeau, D. Span, V. Coppee, J. Dominik, Evolution of the trophic state of Lake Annecy (eastern France) since the last glaciation as indicated by iron, manganese and phosphorus speciation. *J. Paleolimnol.* **25**, 205 (2001). doi:10.1023/A:1008100432461
97. K. A. Koinig, W. Shoty, A. F. Lotter, C. Ohlendorf, M. Sturm, 9000 years of geochemical evolution of lithogenic major and trace elements in the sediment of an alpine lake - the role of climate, vegetation, and land-use history. *J. Paleolimnol.* **30**, 307 (2003). doi:10.1023/A:1026080712312
98. G. H. Haug, K. A. Hughen, D. M. Sigman, L. C. Peterson, U. Röhl, Southward migration of the intertropical convergence zone through the Holocene. *Science* **293**, 1304 (2001). doi:10.1126/science.1059725 Medline
99. G. Yancheva *et al.*, Influence of the intertropical convergence zone on the

- East Asian monsoon. *Nature* **445**, 74 (2007). [doi:10.1038/nature05431](https://doi.org/10.1038/nature05431)
[Medline](#)
100. S. M. Colman *et al.*, Continental climate response to orbital forcing from biogenic silica records in Lake Baikal. *Nature* **378**, 769 (1995). [doi:10.1038/378769a0](https://doi.org/10.1038/378769a0)
101. M. V. Cherapanova, J. A. Snyder, J. Brigham-Grette, Diatom stratigraphy of the last 250 ka at Lake El'gygytgyn, northeast Siberia. *J. Paleolimnol.* **37**, 155 (2007). [doi:10.1007/s10933-006-9019-4](https://doi.org/10.1007/s10933-006-9019-4)
102. H. Cremer, B. Wagner, The diatom flora in the ultra-oligotrophic Lake El'gygytgyn, Chukotka. *Polar Biol.* **26**, 105 (2003).
103. T. C. Johnson, E. T. Brown, J. Shi, Biogenic silica deposition in Lake Malawi, East Africa, over the past 150,000 years. *Palaeogeogr. Palaeoclimatol. Palaeoecol.* **303**, 103 (2011). [doi:10.1016/j.palaeo.2010.01.024](https://doi.org/10.1016/j.palaeo.2010.01.024)
104. S. C. Cande, D. V. Kent, Revised calibration of the geomagnetic polarity time scale for the Late Cretaceous and the Cenozoic. *J. Geophys. Res.* **100**, 6093 (1995). [doi:10.1029/94JB03098](https://doi.org/10.1029/94JB03098)
105. L. J. Lourens *et al.*, Evaluation of the Plio-Pleistocene astronomical timescale. *Paleoceanography* **11**, 391 (1996). [doi:10.1029/96PA01125](https://doi.org/10.1029/96PA01125)
106. R. McKay *et al.*, The stratigraphic signature of the late Cenozoic Antarctic Ice Sheets in the Ross Embayment. *Geol. Soc. Am. Bull.* **121**, 1537 (2009). [doi:10.1130/B26540.1](https://doi.org/10.1130/B26540.1)

Acknowledgments: Drilling operations were funded by the International Continental Scientific Drilling Program (ICDP), the U.S. NSF, the German Federal Ministry of Education and Research (BMBF), Alfred Wegener Institute (AWI) and Helmholtz Centre Potsdam (GFZ), the Russian Academy of Sciences Far East Branch (RAS FEB), the Russian Foundation for Basic Research (RFBR), and the Austrian Federal Ministry of Science and Research (BMWF). The Russian GLAD 800 drilling system was developed and operated by DOSECC Inc. We thank all participants of the expedition for their engagement during recovery of the ICDP 5011-1 cores. Funding of core analyses was provided by BMBF (grant no. 03G0642), German Research Foundation (DFG, grant no. ME 1169/21 and /24), U.S. NSF (grant no. 0602471), Vetenskapsrådet, FORMAS, the Kempe Foundation, and the Civilian Research and Development Foundation (CRDF, grant no. RUG1-2987-MA-10). We are grateful to N. Mantke, A. Shahnazarian, and numerous students (Univ. Cologne) for their competent help in core processing; T. Matrosova for contributing modern surface pollen data; and R. McKay for providing a modified lithological log of the ANDRILL 1B record. We also thank four anonymous reviewers for supportive and constructive comments that greatly improved the manuscript. The data reported in this paper are available in the databases of PANGAEA via www.pangaea.de (doi:10.1594/PANGAEA.783305) and of the U.S. National Climatic Data Center via www.ncdc.noaa.gov/paleo/paleolim/paleolim_data.html.

Supplementary Materials

www.sciencemag.org/cgi/content/full/science.1222135/DC1

Materials and Methods

Supplementary Text

Figs. S1 to S6

Tables S1 to S5

References (57–106)

19 March 2012; accepted 1 June 2012

Published online 21 June 2012

10.1126/science.1222135